

Tin tetrabromide at high pressures: Reversible crystalline-to-amorphous and electronic transitions

W. Williamson III and S. A. Lee

Department of Physics and Astronomy, University of Toledo, Toledo, Ohio 43606

(Received 18 March 1991)

Several phase transitions have been observed in SnBr_4 up to 23 GPa. Measurements of the Raman spectra show that additional modes are observed in the lattice region at about 4 GPa, suggesting that the symmetry of the unit cell is changing. All lattice modes disappear and the internal vibrational modes lose their splitting in the 13–15-GPa region, indicating that a crystal-to-amorphous transition occurs in this pressure range. Upon release of pressure, the amorphous phase is stable to about 1 GPa. A crystalline phase is observed below 1 GPa. Optical absorption experiments indicate that the optical band gap displays a continuous (and reversible) closure with increasing pressure. A photoluminescence signal is observed to red shift with increasing pressure and is quenched in the amorphous state.

I. INTRODUCTION

The properties of the amorphous state and the connection between crystalline and amorphous phases is a subject of considerable interest.^{1–3} Though most amorphous materials have been prepared by rapid cooling of the liquid phase, recent work has shown several interesting phenomena in pressure-induced amorphization.^{4–17} Application of pressure on ice at 77 K produces a high-density amorphous phase at about 1.0 GPa.^{6–9} The production of this phase of ice is related to crossing the extrapolation of the boundary between ice Ih and liquid water, suggesting that this phase transition corresponds to pressure-induced “melting.” Another interesting effect observed in pressure-induced amorphization is the recent observation that certain materials display an amorphous-to-crystal transition upon the release of pressure.^{4,5,13–17} Kruger and Jeanloz have reported that small crystals of AlPO_4 return to the same crystalline phase with the same orientation of axes upon cycling to pressures above 15 GPa.¹⁴

In this paper, we report our study of the molecular crystal SnBr_4 as a function of pressure up to 23 GPa. At ambient pressure, SnBr_4 is a tetrahedral molecule, described by the point group T_d . Brand and Sackmann¹⁸ have determined that the unit cell of SnBr_4 at one atmosphere is monoclinic (space group $P2_1/c$, or C_{2h}^5) with four molecules located on general sites. Several phase transitions, including a reversible crystal-to-amorphous one, have been observed over the pressure range of the experiments reported here. We have also studied the closure of the optical band gap and observed photoluminescence over this same pressure range.

II. EXPERIMENTAL DETAILS

Samples of SnBr_4 were obtained from Aldrich Chemical Co., Inc. SnBr_4 has a melting point of 304 K at atmospheric pressure and is thus a soft crystal under ambient conditions. Powdered SnBr_4 was placed inside a miniature Merrill-Bassett diamond anvil cell which was

used to generate high pressure.¹⁹ The cells were loaded in a nitrogen environment inside a glove bag to prevent contamination. Small chips of ruby were loaded with the SnBr_4 so that standard ruby luminescence measurements could be used to determine the pressure.²⁰ Pressure gradients within the cell were estimated to have been less than 15% at all pressures based on measurements of ruby chips at various locations within the cell. By performing the experiments on small portions of the sample close to a ruby, the errors in the value of the pressure were approximately 0.3 GPa for experiments below 10 GPa and 0.6 GPa for experiments above 10 GPa. All experiments were carried out at room temperature.

Raman and photoluminescence (PL) experiments were performed using an Ar^+ -ion laser. Raman experiments were carried out using 514.5-nm light at powers between 1 and 200 mW. PL data were obtained using both 514.5- and 488.0-nm light over similar power ranges. Backscattered light was collected with a double monochromator. Standard photon counting electronics were employed and the spectra were collected with a microcomputer which also controlled the stepper motor of the monochromator.

Optical absorption (OA) measurements were made by focusing light from a standard lamp through a 400- μm pinhole onto the back of the cell and collecting the transmitted light. The OA spectra were corrected for the response function of the monochromator.

III. RESULTS AND DISCUSSION

Raman studies provide a wealth of information on internal and lattice vibrational modes. The SnBr_4 molecule has four Raman-active internal vibrational modes: the symmetric stretch ν_1 at 220 cm^{-1} , the doubly degenerate deformation ν_2 at 70 cm^{-1} , the triply degenerate stretch ν_3 at 280 cm^{-1} , and the triply degenerate deformation ν_4 at 90 cm^{-1} .^{21–23} Figure 1 shows several typical low-pressure Raman spectra as pressure is increased. Note the changes that occur in the lattice region (~ 30 – 60 cm^{-1} at low pressures) and the internal mode region (> 65 cm^{-1} at low pressures). The error in locating the position of the modes is estimated to be ± 1 cm^{-1}

for the sharp peaks and $\pm 3 \text{ cm}^{-1}$ for the broad peaks. Figure 2 shows the Raman shift of the observed peaks as a function of increasing pressure. The appearance and disappearance of Raman modes at various pressures provides evidence for more than one phase transition.

In a study at one atmosphere, Zeng and Anderson²¹ observed 12 sharp, closely spaced Raman-active lattice modes in the $25\text{--}55 \text{ cm}^{-1}$ region at 20 K. At room tem-

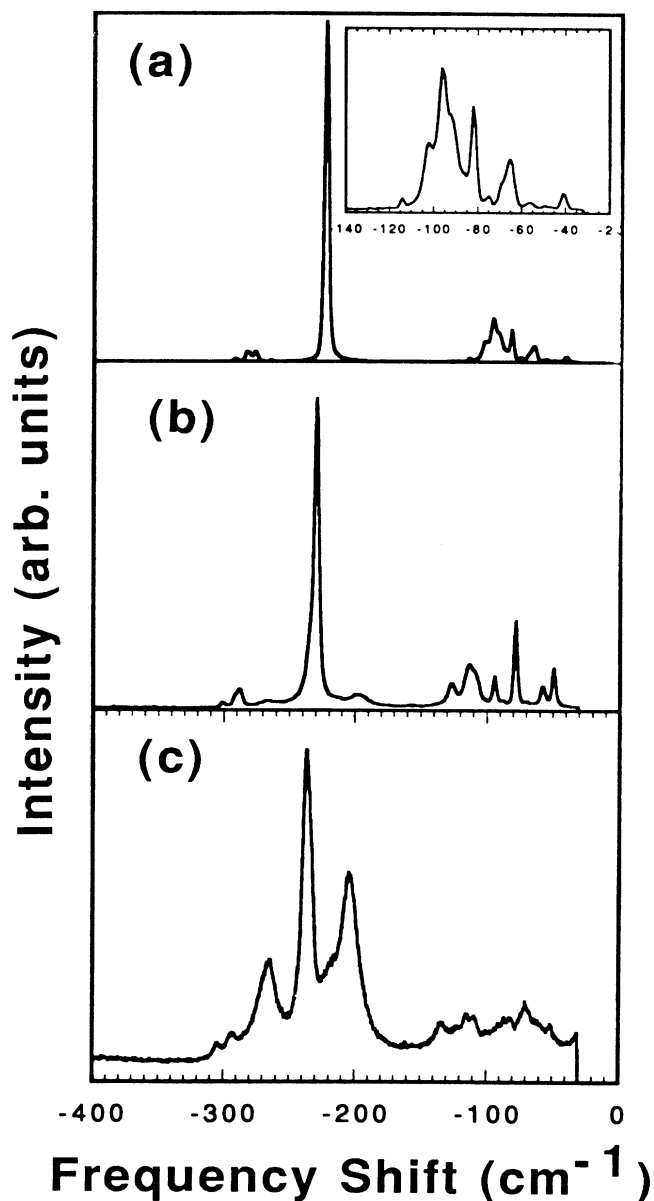


FIG. 1. Typical Raman spectra at (a) 3.0 GPa, (b) 7.2 GPa, and (c) 8.6 GPa for increasing pressure. The inset of (a) shows an expanded view of the low-frequency region of this spectrum.

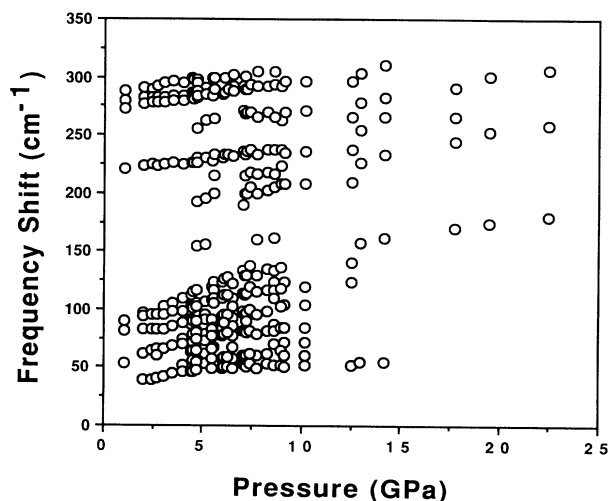


FIG. 2. The pressure dependence of the lattice and internal vibrational modes as the pressure is increased. The error bars for the frequencies are smaller than the size of the symbols. The error bars for the pressure are estimated to be less than 0.3 GPa below 10 GPa and 0.6 GPa above 10 GPa.

perature, thermal effects broaden and overlap these modes. As shown in Fig. 2, a number of new lattice modes are observed as the pressure is increased above about 4 GPa. The change in the number of the lattice modes indicates that a structural phase transition occurs at this pressure. The number of allowed lattice modes is dependent on the number of molecules in the unit cell. Since the number of observed lattice modes is greater above 4 GPa, the unit cell of the high-pressure phase most likely contains more than four molecules (the number of molecules in the unit cell at one atmosphere¹⁸).

Another phase transition is observed in the vicinity of 15 GPa, as is evident from Fig. 2. Above this pressure, none of the lattice modes can be observed, indicating that a crystal-to-amorphous transition has occurred. The Raman spectra of Fig. 3 show the dramatic changes in the lattice region as the transition occurs. Additional evidence for this phase transition is also found in the internal mode region of the Raman spectra.

A dramatic change in the vicinity of the ν_1 mode is first observed at about 5 GPa with the appearance of additional peaks separated by $\sim \pm 30 \text{ cm}^{-1}$, as shown in Figs. 1(b) and 1(c). As the pressure is increased, the intensity of these "satellite" peaks grow relative to the intensity of the ν_1 mode, as displayed in Fig. 4. This figure shows that the satellite modes are significantly more intense than the ν_1 mode above 13 GPa. The fact that these two satellite peaks are symmetrically shifted with respect to the ν_1 mode suggests that these modes represent a splitting of the ν_1 mode. A Mössbauer study of SnI_4 by Pasternak and Taylor¹³ showed that these molecules form chains in the amorphous phase. These chains are formed by bonding between halogen atoms on neighboring molecules. This would provide for coupling between the normal modes of vibrations of the molecular

units and result in a splitting of the ν_1 mode into two A_g modes. This is consistent with our observations for SnBr_4 and the observations of Sugai⁵ for SnI_4 .

This suggestion for the origin of the A_g modes implies that the relative intensities of the A_g and ν_1 modes can be used to estimate the relative amounts of the crystalline and amorphous phases. As shown in Fig. 4, the two phases coexist in the pressure range between 5 and 18 GPa. For increasing pressure, the sample changes from predominantly crystalline to predominantly amorphous near 13 GPa. This observation is consistent with the observation that the lattice modes are not observed in the Raman spectra above about 15 GPa. Substantial hysteresis is observed for the amorphous phase as the pres-

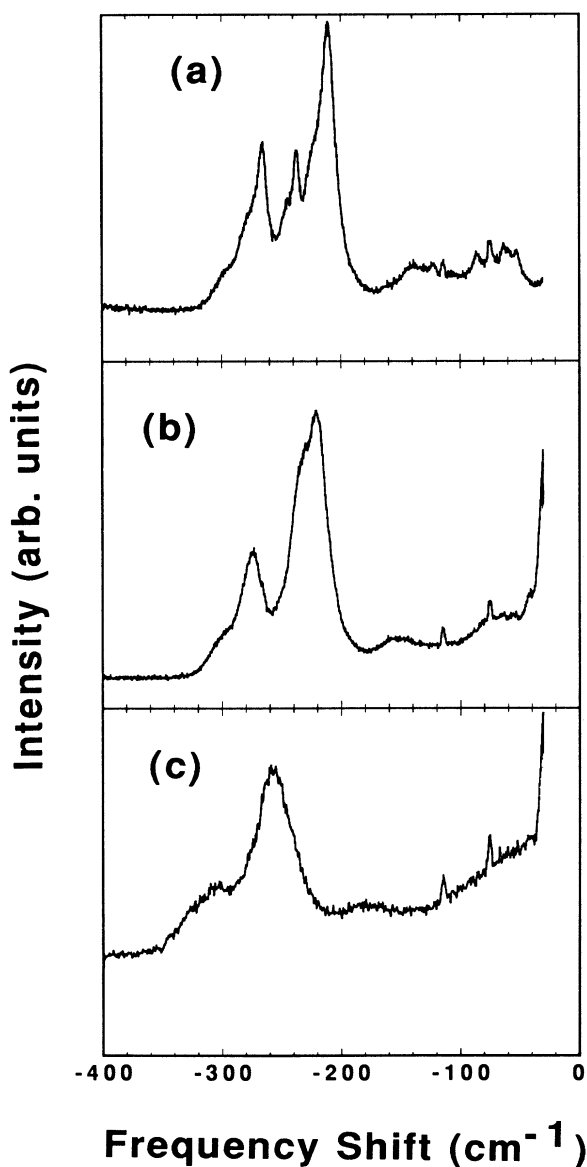


FIG. 3. Typical Raman spectra at (a) 12.6 GPa, (b) 13.0 GPa, and (c) 22.5 GPa for increasing pressure. Plasma lines are at 77 and 117 cm^{-1} .

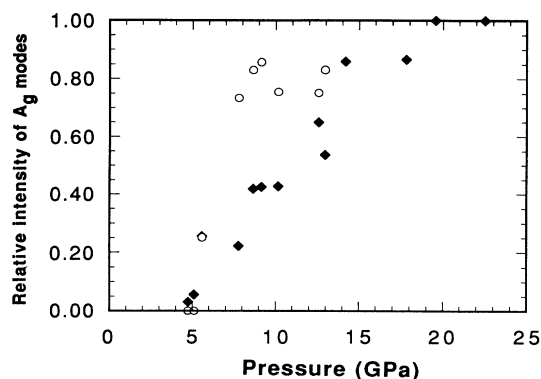


FIG. 4. Intensity of the A_g modes relative to the intensity of the ν_1 mode as a function of pressure. The solid diamonds (\blacklozenge) are for increasing pressure and the circles (\circ) are for decreasing pressure.

sure is decreased. Figure 4 shows that a large fraction of the molecular units remain in chains until about 6 GPa.

In Fig. 5, the frequency of the observed Raman peaks is plotted as a function of decreasing pressure. A comparison of Figs. 5 and 2 shows substantial pressure hysteresis. A lattice mode is not observed until the pressure on the sample is decreased to 0.62 GPa (as shown in Fig. 6), implying that an amorphous-to-crystal transition occurs near this pressure. Additional evidence for such a transition is displayed in Fig. 7. At 1.17 GPa, all of the internal modes are broad, characteristic of the amorphous state. The ν_2 and ν_4 modes overlap into one very broad peak. Also, the ν_3 mode is a very broad peak with no splitting. At 0.62 GPa, all of the internal modes have

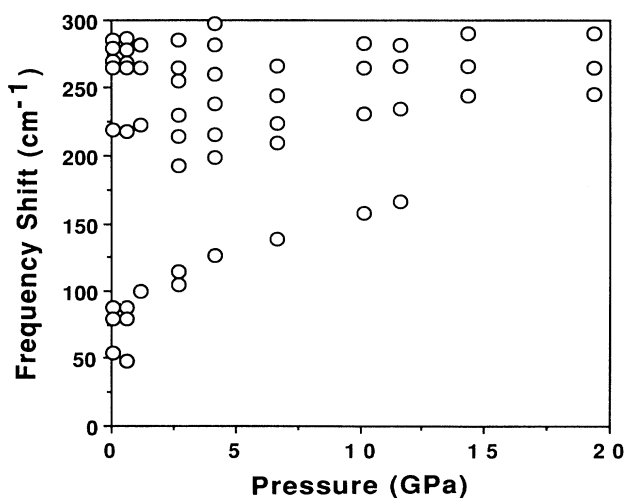


FIG. 5. The pressure dependence of the lattice and internal vibrational modes as the pressure is decreased. The error bars for the frequencies are smaller than the size of the symbols. The error bars for the pressure are estimated to be less than 0.3 GPa below 10 GPa and 0.6 GPa above 10 GPa.

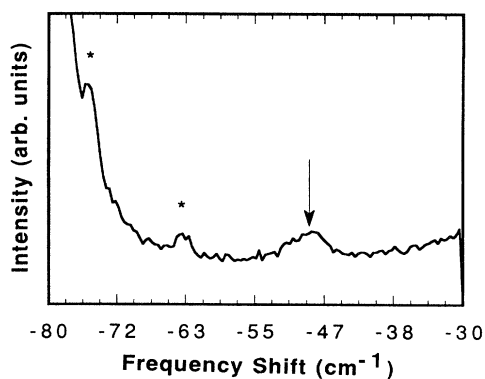


FIG. 6. Lattice mode region of the Raman spectrum of SnBr_4 at 0.62 GPa after being cycled above 18 GPa. The presence of a lattice mode at 48 cm^{-1} indicates that the sample has returned to a crystalline phase. Plasma lines are denoted by asterisks.

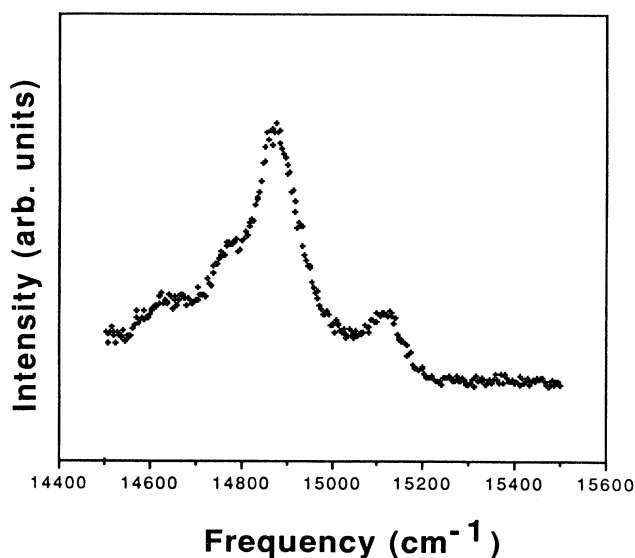


FIG. 8. Typical photoluminescence spectrum at 4.7 GPa.

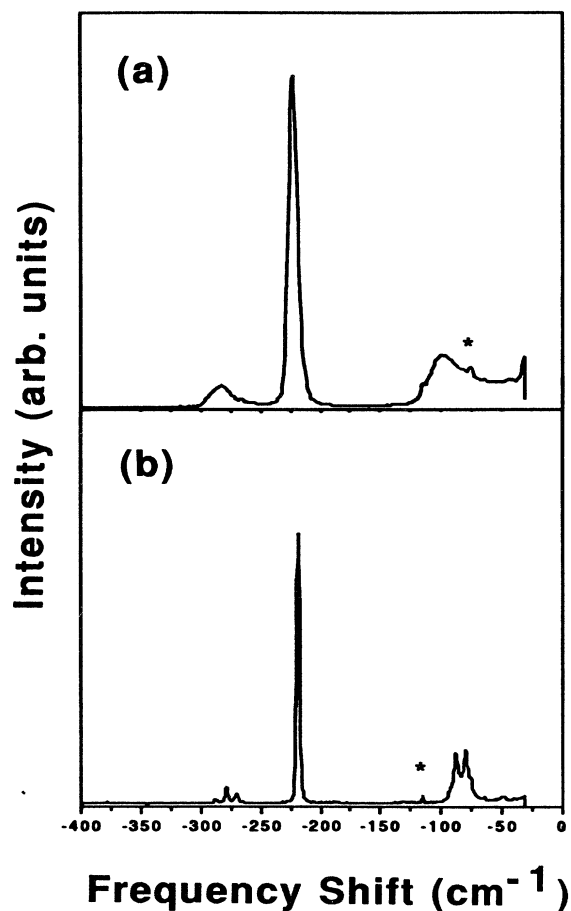


FIG. 7. Raman spectra at (a) 1.17 GPa and (b) 0.62 GPa for decreasing pressure. The splitting and narrowing of the internal modes indicate the return to a crystalline phase at 0.62 GPa. Plasma lines are denoted by the asterisks.

narrowed and show the splitting characteristic of the crystalline phase.

In addition to investigating vibrational characteristics via Raman spectroscopy, measurements were also made of the electronic properties by observing photoluminescence and optical absorption of SnBr_4 . Figure 8 shows a typical PL spectra with three peaks and one shoulder. At all pressures at which PL is observed, the spectra had the same characteristic shape. No changes were observed in the number of peaks, their relative intensities, or the frequency separation of the peaks. The PL was observed in

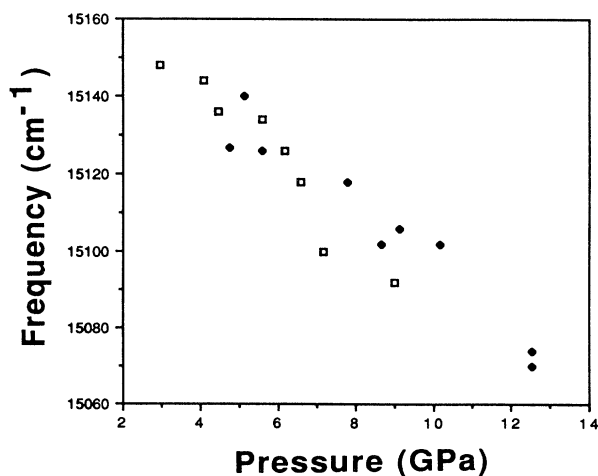


FIG. 9. The position of the highest-frequency photoluminescence peak as a function of pressure. The solid diamonds (◆) are for increasing pressure and the squares (□) are for decreasing pressure. The error bars for the frequency are smaller than the size of the symbols. The error bars for the pressure are estimated to be less than 0.3 GPa below 10 GPa and less than 0.6 GPa above 10 GPa.

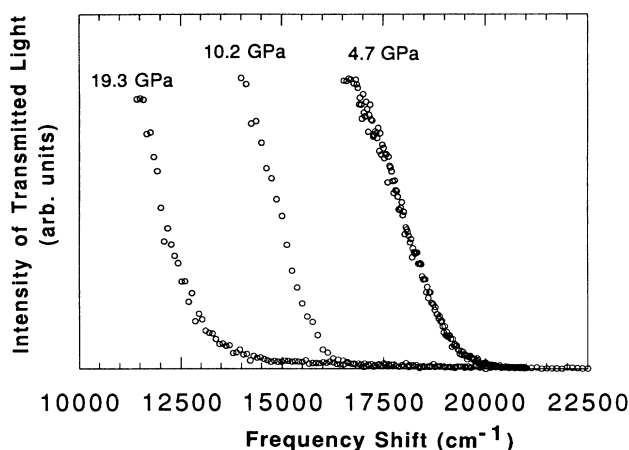


FIG. 10. Transmission spectra of 4.7 GPa, 10.2 GPa, and 19.3 GPa, showing the closure of the optical band gap as the pressure is increased.

crystalline samples and found to red shift slightly as pressure was increased, as shown in Fig. 9.

The band gap was measured by optical absorption experiments. As shown in Fig. 10, a band edge is observed in the transmission spectra. The point of inflection of these spectra as a function of pressure is plotted in Fig. 11 along with the frequency of the highest-energy PL peak. The optical band gap is found to close monotonically with increasing pressure. Very little hysteresis is observed for the pressure dependence of the optical band gap. At the highest pressures of these experiments, the band gap was in the ir, below the range of sensitivity of our experimental apparatus.

For pressures below about 13 GPa, the optical band gap is larger than the energy of the PL. At low pressures, the optical band gap is *substantially* larger than the energy of the PL. The PL signal has a much smaller red shift as a function of pressure than the optical band gap, indicating that the states involved in the PL are relatively insensitive to pressure. When the pressure on the sample exceeded about 13 GPa, the PL could no longer be observed. Figure 11 shows that this is the pressure at which the optical band gap becomes smaller than the energy of the PL. This would quench the PL. However, the crystal-to-amorphous transition also occurs at this pressure. Upon decreasing the pressure, the PL was not observed while the sample was still amorphous (above ~ 1 GPa). This is presumably due to the presence of gap states in the amorphous phase which provide a nonradiative mechanism for the electrons to return to the valence band.

IV. CONCLUSIONS

Investigation of vibrational and electronic properties of SnBr_4 reveal several pressure-induced phase transitions.

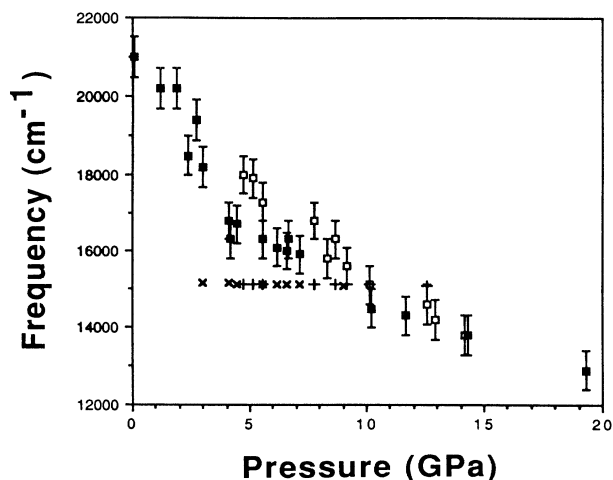


FIG. 11. The pressure dependence of the optical band gap and the frequency of the highest-energy photoluminescence peak. For the optical band gap, the solid squares (\blacksquare) are for increasing pressure and the open squares (\square) are for decreasing pressure. The error bars for the optical band gap are shown. For the photoluminescence peak, the pluses (+) are for increasing pressure and the \times 's are for decreasing pressure. The error bars for the photoluminescence are much smaller than the symbols. The error bars for the pressure are estimated to be less than 0.3 GPa below 10 GPa and 0.6 GPa above 10 GPa.

At about 4 GPa, an increase in the number of observed lattice modes and a splitting of some of the internal modes indicates a change in the symmetry of the unit cell. Above 5 GPa, a splitting of the ν_1 mode into two $2A_g$ breathing modes is observed, marking the onset of a transition involving the molecular units. By 13 GPa these A_g modes dominate the spectra. Above 15 GPa, the lattice modes are no longer observed, showing that a crystal-to-amorphous transition has occurred. The amorphous phase is believed to consist of randomly oriented chains of SnBr_4 . Upon the release of pressure, the chains are stable to below 6 GPa while the amorphous phase is stable to below 1 GPa. A crystalline phase is observed at 0.62 GPa, indicating that an amorphous-to-crystal transition has occurred. The optical band gap is observed to close as a function of increasing pressure. A photoluminescence signal is observed in the crystalline phase below 13 GPa. Due to the large difference in the band gap and the photoluminescence energy at low pressure, the photoluminescence is due to states deep in the band gap. This photoluminescence signal displays a small red shift as the pressure is increased and is not observed in the amorphous phase.

ACKNOWLEDGMENT

We thank A. Anderson for suggesting SnBr_4 as a material of interest.

- ¹S. R. Elliott, *Physics of Amorphous Materials*, 2nd ed. (Wiley, New York, 1990).
- ²*Physics of Disordered Materials*, edited by D. Adler, H. Fritzsche, and S. R. Ovshinsky (Plenum, New York, 1985).
- ³R. Zallen, *The Physics of Amorphous Solids* (Wiley, New York, 1983).
- ⁴Y. Fujii, M. Kowaka, and A. Onodera, *J. Phys. C* **18**, 789 (1985).
- ⁵S. Sugai, *J. Phys. C* **18**, 799 (1985).
- ⁶O. Mishima, L. D. Calvert, and E. Whalley, *Nature* **310**, 393 (1984).
- ⁷D. D. Klug, O. Mishima, and E. Whalley, *Physica B* **139&140**, 475 (1986).
- ⁸D. D. Klug, O. Mishima, and E. Whalley, *J. Chem. Phys.* **86**, 5323 (1987).
- ⁹D. D. Klug, Y. P. Honda, J. S. Tse, and E. Whalley, *J. Chem. Phys.* **90**, 2390 (1989).
- ¹⁰K. M. Yenice, S. A. Lee, and D. W. Downs, *Mol. Phys.* **69**, 973 (1990).
- ¹¹S. A. Lee, A. Anderson, S. M. Lindsay, and R. C. Hanson, *High Pres. Res.* **3**, 230 (1990).
- ¹²K. M. Yenice and S. A. Lee, in *Proceedings of the Twelfth International Conference on Raman Spectroscopy*, edited by J. R. Durig and J. F. Sullivan (Wiley, Chichester, 1990), p. 516.
- ¹³M. Pasternak and R. D. Taylor, *Phys. Rev. B* **37**, 8130 (1988).
- ¹⁴M. B. Kruger and R. Jeanloz, *Science* **249**, 647 (1990).
- ¹⁵F. E. A. Melo, V. Lemos, F. Cerdeira, and J. M. Filho, *Phys. Rev. B* **35**, 3633 (1987).
- ¹⁶H. Sankaran, S. K. Sikka, S. M. Sharma, and R. Chidambaram, *Phys. Rev. B* **38**, 170 (1988).
- ¹⁷M. B. Kruger, Q. Williams, and R. Jeanloz, *J. Chem. Phys.* **91**, 5910 (1989).
- ¹⁸V. P. Brand and H. Sackmann, *Acta Crystallogr.* **16**, 446 (1963).
- ¹⁹A. Jayaraman, *Rev. Sci. Instrum.* **57**, 6 (1986).
- ²⁰H. K. Mao, P. M. Bell, J. W. Shaner, and D. J. Steinberg, *J. Appl. Phys.* **49**, 3276 (1978).
- ²¹W. Y. Zeng and A. Anderson, *J. Raman Spectrosc.* **18**, 327 (1987).
- ²²G. Herzberg, *Infrared and Raman Spectra* (Van Nostrand, Princeton, 1945).
- ²³J. A. Creighton and T. J. Sinclair, *Spectrochim. Acta* **35A**, 137 (1979).